# Mapping urban green space of the 36 major cities in China using ZY-3 satellite images based on a feature robust to low-brightness pixels

Chen Lu [1], Xiaoyu Du [2], Guanghui Wang [3], Wei Zhang [4], Lijuan Zheng [5]

[1] Land Satellite Remoting Sensing Application Center, Ministry of Natural Resource, Beijing, China - alasluchen@sina.com
[2] School of Environment and Spatial Informatics, China University of Mining and Technology, Xuzhou, China - 312748063@qq.com
[3] Land Satellite Remoting Sensing Application Center, Ministry of Natural Resource, Beijing, China – 254197594@qq.com
[4] Land Satellite Remoting Sensing Application Center, Ministry of Natural Resource, Beijing, China - dave6806@163.com
[5] Land Satellite Remoting Sensing Application Center, Ministry of Natural Resource, Beijing, China - zhenglijuan1022@163.com

**Keywords:** Urban Green Spaces, Mapping, Spatial Pattern, China, ZY-3 Satellite.

**Abstract**

Urban green spaces (UGS), integral to modern urban life, play a pivotal role in shaping ecological, low-carbon, resilient, and livable cities. Understanding the microstructure and macro patterns of UGS is necessary but limited. In this context, we investigated the spatial patterns in the 36 major cities in China using Ziyuan-3 remote sensing images. We used a method for extracting UGS suitable for complex urban environments, and then selected 5 landscape pattern indices such as percent of landscape and patch density to analyse the spatial pattern of UGS in the 36 cities. The results show that: (1) The overall accuracy, recall, F1 value, and intersection over union of the extraction results of UGS were 94.62%, 94.11%, 94.36%, and 89.33% respectively; (2) Overall, the green space rate of the 36 cities exhibited a spatial distribution pattern of “high in the east and low in the west, low in the north and high in the south”; (3) Variations among cities were weak in terms of patch shape, but significant in patch density. The findings of this study cater to the escalating demands of urban planning and management.

## 1. Introduction

Urban green space (UGS), characterized by natural and artificial vegetation, constitutes indispensable landcovers in urban areas. UGSs play a crucial role in improving urban ecological environment, due to their ability to reduce air pollution, mitigate dust, and alleviate the urban heat island effect. Moreover, UGSs have a positive impact on mental well-being and physical health, providing relief from stress and promoting overall wellness among residents (Chen et al. 2022). Simultaneously, UGSs enhance the quality of urban living by serving as recreational, exercise, and social spaces, thereby contributing to residents' happiness (Richards and Belcher 2019). UGSs are an indispensable component of cities, and accurately and efficiently monitoring their extent is of paramount importance for evaluating urban ecological environment and optimizing urban structures.

Traditionally, acquiring the spatial distribution of UGSs relied on manual field measurements, resulting in high data accuracy. However, due to the extensive and fragmented coverage of UGSs, manual surveys are inefficient and resource-intensive (Liao et al. 2021). Meeting the demands for frequent updates of UGS spatial distributions using manual field measurements is challenging. Advancements in Earth observation satellites have led to the widespread use of medium-resolution and low-resolution remote sensing images for UGS extraction (Yin et al. 2022; Kuang and Dou 2020). However, medium-resolution and low-resolution remote sensing images were limited to extracting large patches of UGS or estimated the proportion of green spaces with a pixel. High-resolution remote sensing images enabled the extraction of small green patches in street blocks and green belts, facilitating large-scale monitoring of fine distributions of UGSs (Zhang et al. 2023).

The utilization of remote sensing images has gained popularity in studying the patterns and dynamics of UGSs. Through the analysis of medium-resolution images from satellites such as Landsat, researchers can map and monitor the changes of UGSs over time. Researchers had been conducted in several cities in China, including Beijing, Wuhan, Shenzhen, Guangzhou, and Shanghai, aiming to explore the quantity, quality, and spatial distribution of UGSs (Huang et al. 2017, 2021; Yin et al. 2022). These investigations have revealed a decline in UGSs across multiple cities due to urbanization, economic development, and population growth. However, there had also been instances of an expansion in UGSs, especially in central urban areas. Furthermore, the relationship between green spaces and urban heat island effect had been examined, with results showing that green spaces can help mitigate the effects of urbanization on temperature (An et al. 2022; Qiao et al. 2020). In summary, the use of remote sensing images had provided valuable insights into the patterns and dynamics of UISs, contributing to the planning and management of sustainable cities. However, our understanding of the fine-scale distribution of UGSs remains limited.

The objective of this study was to was to efficiently acquire large-scale spatial data on urban green spaces (UGSs) in China’s 36 major cities using ZY-3 satellite images. We extracted green spaces both inside and outside of building shadows using different features. Subsequently, we selected five landscape pattern indices to analyse the spatial distribution of urban green spaces across 36 cities. The findings from this

analysis contribute to urban planning, ecological environment conservation, and the well-being of residents.

## 2. Study area and data

### 2.1 Study area

The study was conducted in the urban areas of China’s 36 major cities, including four municipalities, 27 provincial capitals, and five municipalities with independent planning status. The 36 cities located in different regions of China (Figure 1) were grouped into three levels according to the urban population: level I (greater than 10 million, 7 cities), level II (5 million to 10 million, 12 cities), and level III (<5 million, 17 cities).

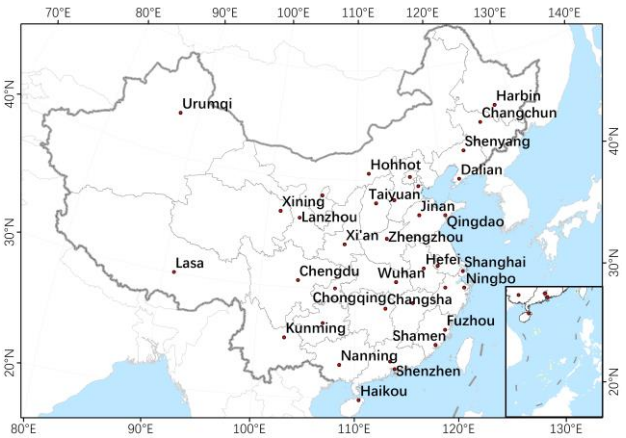


Figure 1. Map of study area

### 2.2 Data sources

The high-resolution remote sensing images acquired from China's Ziyuan-3 satellite were employed to produce digital ortho-photo maps (DOMs) through a series of preprocessing steps, including orthorectification, geometric correction, and mosaicking. The produced DOMs had a spatial resolution of 2.1 meters and consisted of 4 bands: blue, green, red, and near infrared. Despite variations in the acquisition dates of remote sensing images, all utilized images were obtained in 2023. After producing the DOMs, the maps were utilized to extract UISs in the study area.

Auxiliary data included urban and administrative boundaries in this study. The global urban boundary and prefecture-level administrative unit were employed to limit extraction areas. The urban extent data of the 36 cities was obtained from the multi-temporal dataset of global urban boundaries (GUB, Li et al. 2020). We removed the patches that were smaller than 1 $km^2$ in the GUB dataset. The global administrative area was utilized for mapping extraction results.

| Data usage | Data name | Data type |
|---|---|---|
| Remote sensing image | ZY-3 satellite images | Raster, 2.1m |
| Auxiliary data | Global urban boundary | Vector |
| | Prefecture-level administrative unit | Vector |
| | Global administrative area | Vector |

Table 1. Data details

## 3. Method

The flowchart of this study is shown in Figure 2, which is divided into 2 parts: (1) using different features to extract UGSs in non-shadow and shadow areas, and (2) calculating landscape pattern indices to analyse the spatial distribution characteristics of UGSs.

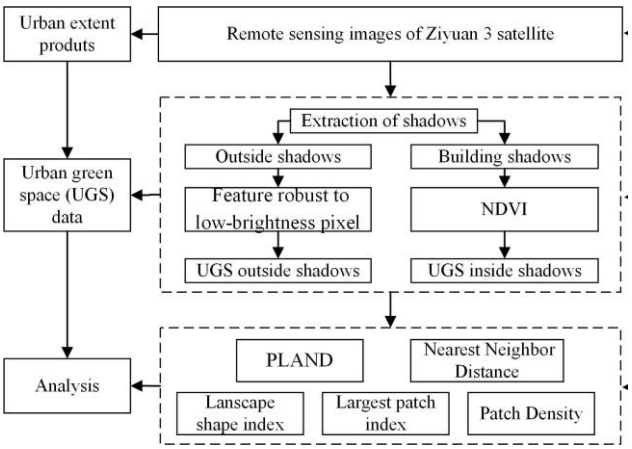


Figure 2. Extraction and analysis process of urban green spaces

### 3.1 Extraction of UGS

#### 3.1.1 Feature for extracting shadows

First, the SAM (Segment Anything Model) was used to segment a remote sensing image, and then the image was converted to the HSI color space to calculate the features for extracting shadows. These features were then statistically analysed to generate object-level shadow extraction features. Figure 3 shows the flowchart of calculating the object-level feature for extracting shadows.

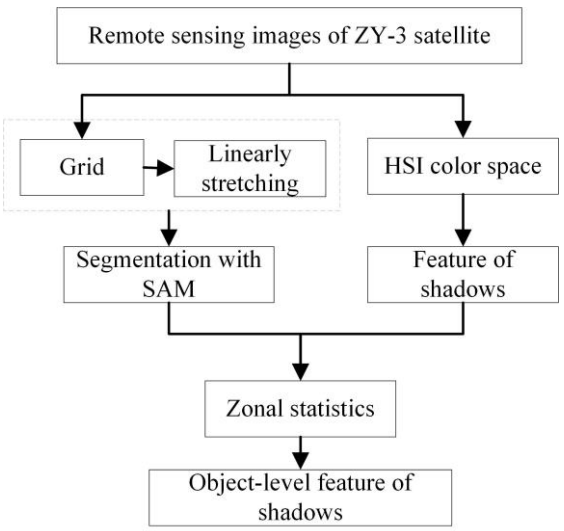


Figure 3. Flowchart of calculating the object-level features for extracting shadows

The images of study areas were cropped using a window of 256x256 pixels with a 20% overlap between adjacent windows. The tones of the used remote sensing images were overall dark, so the percentage linear stretch was applied to the cropped images, which significantly enhanced the brightness and improved the distinguishability of shadow areas.

In the HSI color space, shadow areas were characterized by higher hue and saturation, but lower brightness. Based on this, the shadow extraction feature $F_S$ in the HSI color space was calculated as follows:

$$F_S = \frac{H + S}{I} \quad (1)$$

where $H$ = hue
$S$ = saturation
$I$ = brightness

Using the segmented objects from the SAM model as statistical units, the average values of the feature $F_S$ were calculated to generate object-level features for shadow extraction.

#### 3.1.2 Feature for extracting greens

In order to enhance the distinction between vegetation and water, we improved NDVI according the spectral characteristics of green spaces and water bodies in ZY-3 satellite images. The green space extraction feature $F_G$ that was resistant to the interference of low-brightness pixels was constructed by increasing the ratio of the numerator to the denominator as follows:

$$F_G = \frac{(NIR - R)(NIR - R)}{(NIR + R)} \quad (2)$$

where $NIR$ = value of near infrared band
$R$ = value of red band

#### 3.1.3 Extraction process

The entire process of extracting UGSs proceeded as follows: first, we extracted building shadows; next, we identified green spaces both outside and inside these shadows; and finally, we merged the green spaces from both areas. The thresholds for the UGS extraction of each image were determined through manual interpretation. The extraction was carried out for each city, generating extraction results for the 36 cities.

### 3.2 Analysis of UGS

In terms of area, number, density, isolation, and shape, the total of 5 landscape metrics were calculated separately to evaluate landscape structure of UGSs for each city. First, the percentage of landscape (PLAND) were calculated to measure the regional divergence of the area of UGSs. Then, the patch density (PD), the number of patches per unit area of urban areas, was calculated. The largest patch index (LPI) was used to measure the dominance of a single largest patch within UGSs. Furthermore, the Average Nearest Neighbour (ANN) was adapted to quantify distribution of UGS patches. Cities with lower ANN means that UGSs patches were more clustering. In order to measure the complexity of patch shapes of UGSs, the area landscape shape index (LSI) was used. Cities with higher LSI values have more irregular patch shapes of UGSs.

## 4. Results

### 4.1 Overall accuracy

The overall accuracy, recall, and F1 value of the extraction results of UGS were 94.62%, 94.11%, 94.36%, and 89.33% respectively. The mean intersection over union was 89.33%. The mean overall accuracy of classification met the suggested accuracy for land cover analysis, i.e., 85%. Figure 4 is the extraction result of UGS in Shenzhen, with good extraction performance for both large and small green spaces.

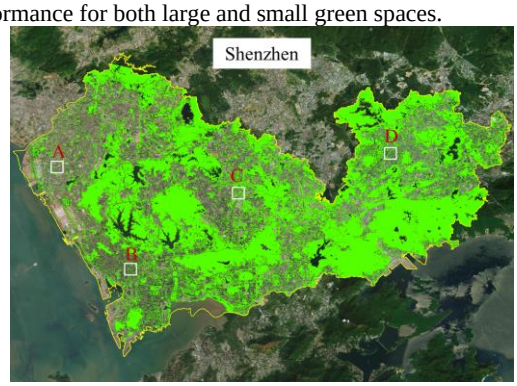


(a) overall result

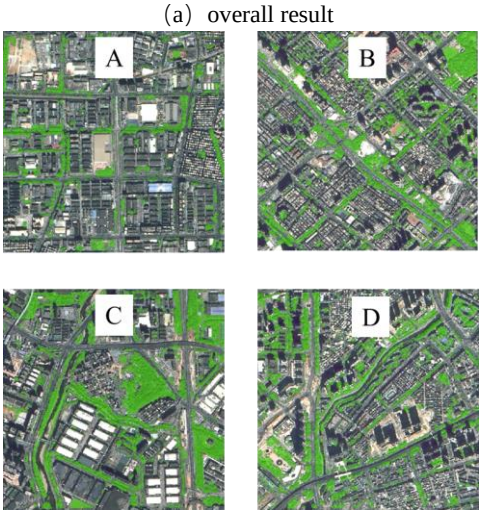


(b) local result

Figure 4. Urban green spaces of Shenzhen.

### 4.2 Analysis of PLAND

The top 10 cities, with the highest PLAND of UGS at the city level, were derived and ranked (Table 2). Among these cities, the highest PLAND of UGS was in Shenzhen. The PLAND of Lhasa was the lowest, with 8.40%. The PLAND of Shenzhen was 5.54 times that of Lhasa. Meanwhile, among the top 10 cities, 8 cities were in the east zones, and only Wuhan and Zhengzhou were in the central zones.

| City | Urban area ($km^2$) | Green space ($km^2$) | PLAND |
|---|---|---|---|
| Shenzhen | 1350.53 | 658.17 | 48.73% |
| Beijing | 1892.55 | 826.55 | 43.67% |
| Xiamen | 629.01 | 263.51 | 41.89% |
| Zhengzhou | 758.05 | 312.17 | 41.18% |
| Jinan | 1008.31 | 409.05 | 40.57% |
| Shanghai | 1532.69 | 588.54 | 38.40% |
| Hangzhou | 1012.92 | 379.76 | 37.49% |
| Shenyang | 731.35 | 273.28 | 37.37% |
| Ningbo | 712.99 | 265.59 | 37.25% |
| Wuhan | 1162.79 | 424.96 | 36.55% |

Table 2. Top 10 cities with highest PLAND

Ranking PLAND in descending order, the cities with large differences in overall PLAND and block-level PLAND are listed in Table 3. Although Guangzhou and Nanchang ranked lower in overall PLAND, the block-level PLAND of the two cities were high. Especially, Guangzhou ranked first in block-level PLAND and 18th in overall PLAND. In contrast, Shenzhen ranked first in overall PLAND of UGS, but 12th in block-level PLAND of UGS.

| City | Rank | Rank of green spaces in blocks | Change |
|---|---|---|---|
| Guangzhou | 18 | 1 | 17 |
| Haikou | 29 | 16 | 13 |
| Chengdu | 19 | 11 | 8 |
| Nanchang | 16 | 9 | 7 |
| Shijiazhuang | 30 | 26 | 4 |
| Nanjing | 12 | 20 | -8 |
| Jinan | 5 | 15 | -10 |
| Xiamen | 3 | 13 | -10 |
| Guiyang | 21 | 32 | -11 |
| Shenzhen | 1 | 12 | -11 |

Table 3. Rank of green spaces in blocks

Certain cities, such as Xining, Guiyang, and Dalian, had a lower overall PLAND of UGS, but a higher PLAND of urban park green space (Table 4). Citizen in these cities could enjoy good green environment by going to parks. On the other hand, there were also cities (Shanghai and Wuhan) where the PLAND of urban park green space ranked lower, but the block-level PLAND of UGSs ranked higher, indicating that citizen can enjoy good green environment in their living blocks.

| City | Rank | Rank of green spaces in parks | Change |
|---|---|---|---|
| Shanghai | 6 | 26 | -20 |
| Wuhan | 10 | 29 | -19 |
| Nanchang | 16 | 33 | -17 |
| Ningbo | 9 | 25 | -16 |
| Shenyang | 8 | 22 | -14 |
| Changsha | 11 | 24 | -13 |
| Dalian | 17 | 4 | 13 |
| Huhehaote | 33 | 18 | 15 |
| Guiyang | 21 | 6 | 15 |
| Xining | 32 | 13 | 19 |

Table 4. Rank of green spaces in parks

Figure 5 shows the spatial distribution of PLAND values of UGS for the 36 Chinese cities. Overall, the cities in the northwest side of the Aihui-Tengchong Line had a lower PLAND of UGS. The five cities with lowest PLAND (Lhasa, Urumqi, Lanzhou, Hohhot, and Xining) were all located in the western region of China. Among the cities in the southeast side of the Aihui-Tengchong Line, there was no clear correlation between latitude and PLAND of UGS. Shenzhen has the highest PLAND, while Beijing and Jinan in North China had a higher PLAND than Xiamen, Guangzhou, and Fuzhou in South China. However, there was a large difference in PLAND of China among northern cities, with both high PLAND in Beijing and low PLAND in Shijiazhuang and Qingdao. The difference in PLAND of UGS among the 4 cities in Northeast China was small.

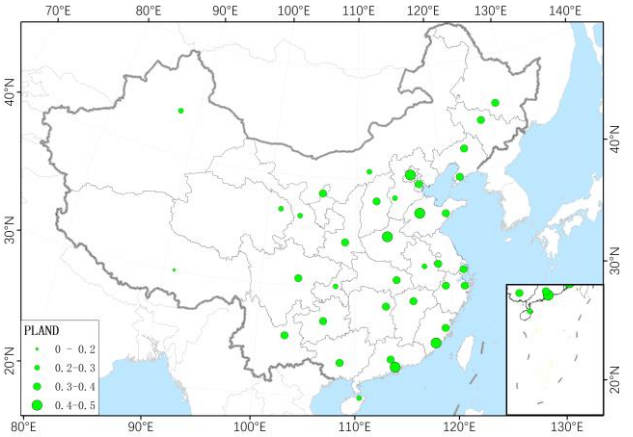


Figure 5. Overall PLAND of UGS

Figure 6 shows the spatial distribution of PLAND values of UGS in blocks for the 36 Chinese cities. Only considering the green space in urban blocks, the PLANDs of in western cities of China remained lower. Yinchuan, Chengdu, and Xi'an were the cities with relatively high block-level PLAND in the western region, and only Yinchuan was far away from the Aihui-Tengchong Line. Among the cities in the southeast side of the Aihui-Tengchong Line, UGS showed a certain latitudinal zonality. The cities along the Yangtze River (Shanghai, Nanjing) and the cities in South China (Xiamen, Fuzhou, Shenzhen, Guangzhou) had relatively high PLAND of urban blocks, while cities in Northeast China (Harbin, Shenyang, Changchun) and cities in North China (Dalian, Shijiazhuang, Tianjin) had lower green space ratios in blocks.

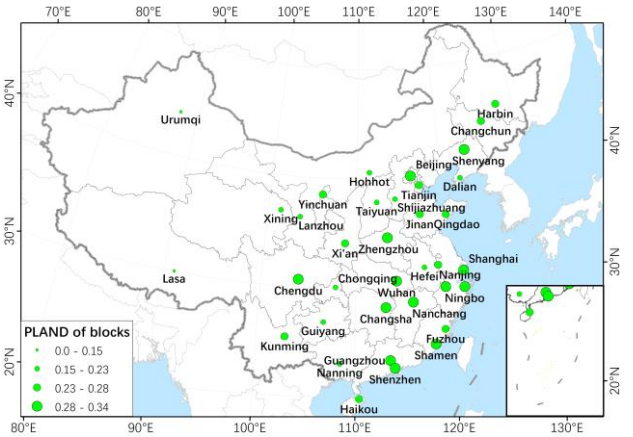


Figure 6. PLAND of UGSs in blocks

Figure 7 shows the spatial distribution of PLAND values of urban park green spaces for the 36 Chinese cities. The cities with the highest proportion of urban park green spaces were Beijing, Dalian, Jinan, Guangzhou, Shenzhen, and Guiyang, with both northern and southern cities represented. At the same

time, Yinchuan, Hohhot, and Xining in the western region had a high PLAND of urban park green spaces.

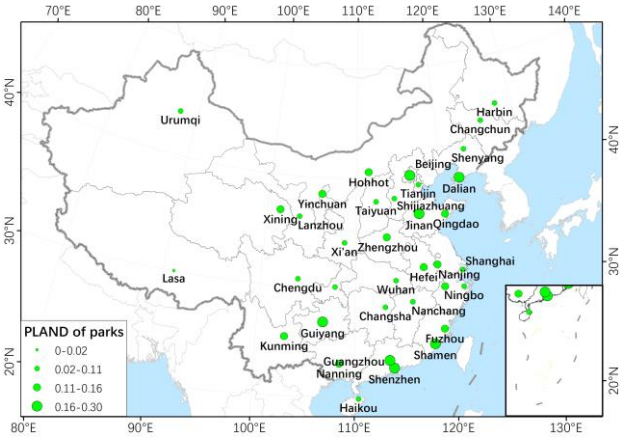


Figure 7. PLAND of urban park green spaces

### 4.3 Analysis of landscape

Landscape metrics of UGSs for the 36 Chinese cities were shown in Figure 8. The mean LPI was 4.34% (SD = 1.12%), ranging from 0.24% to 4.77%. The values suggested that the dominance of the largest UGS patches is weak in most cities and variation is high among these cities. The mean PD was 325.55 count/km$^2$ (SD = 188.46 count/km$^2$), ranging from 111.89 to 1545.96 count/km$^2$. This wide range of PD values indicated that levels of fragmentation of UGS varied greatly in studied cities. The mean LSI of UGSs in blocks of was 1.37 (SD = 0.01), ranging from 1.54 to 1.22. The shape complexity of UGS did not vary much across cities. The ANN values of UGSs in blocks varied from 0.59 to 0.87, averaging (0.06), which showed clustering distribution of UGS patches in these cities.

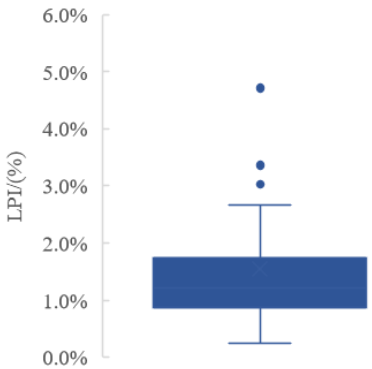


(a)

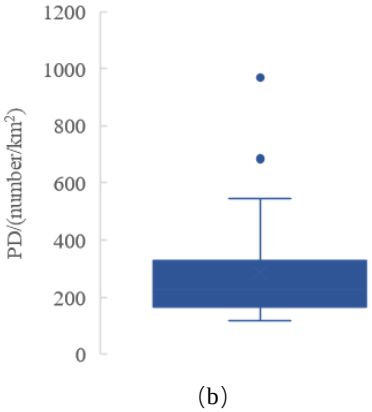


(b)

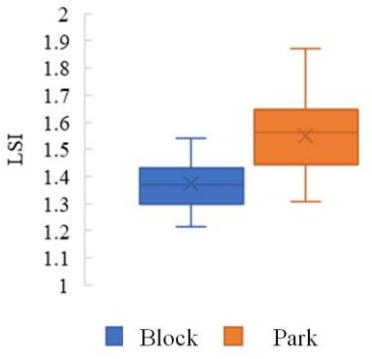


(c)

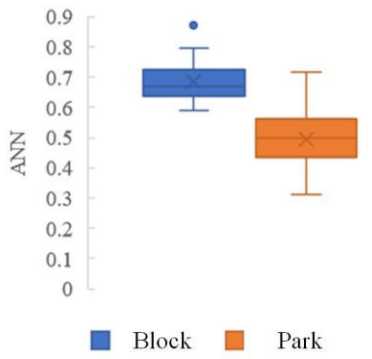


(d)

Figure 8. Summary statistics of landscape metrics of urban green spaces, (a) largest shape index, (b) patch density, (c) landscape shape index, and (d) average nearest neighbour.

## 5. Conclusion

In this study, we employed ZY-3 satellite images to investigate the spatial patterns of UGSs in the 36 major cities. The overall accuracy, recall, F1 value, and intersection over union of the extraction results of UGS were 94.62%, 94.11%, 94.36%, and 89.33% respectively. We found that the Aihui-Tengchong Line divided the western cities of fewer UGSs and the eastern cities of more UGSs. While variations in patch shape were minimal among cities, significant differences existed in patch density and area proportions. The findings of this study addressed to the increasing demands of urban planning and management. In our feature study, we plan to conduct UGS mapping in all cities of China using ZY-3 satellite images.

**Acknowledgements**

This work was financially supported by the National Key Research and Development Program of China: Intelligent extraction and development potential assessment technology of wind power and photovoltaic power station target information (N0.2022YFF1303405) and Rapid identification, evaluation and early warning technology of safety elements on spatial planning (N0.2023YFC3804003).

**References**

An, H., H. Cai, X. Xu, Z. Qiao, and D. Han, 2022: Impacts of Urban Green Space on Land Surface Temperature from Urban Block Perspectives. *Remote Sensing*, 14, 4580, https://doi.org/10.3390/rs14184580.

Chen, B., S. Wu, Y. Song, C. Webster, B. Xu, and P. Gong, 2022: Contrasting inequality in human exposure to greenspace between cities of Global North and Global South. *Nat Commun*, 13, 4636, https://doi.org/10.1038/s41467-022-32258-4.

Huang, C., J. Yang, H. Lu, H. Huang, and L. Yu, 2017: Green Spaces as an Indicator of Urban Health: Evaluating Its Changes in 28 Mega-Cities. *Remote Sensing*, 9, 1266, https://doi.org/10.3390/rs9121266.

N. Clinton, L. Yu, H. Huang, I. Dronova, and J. Jin, 2021: Mapping the maximum extents of urban green spaces in 1039 cities using dense satellite images. *Environ. Res. Lett.*, 16, 064072, https://doi.org/10.1088/1748-9326/ac03dc.

Kuang, W., and Y. Dou, 2020: Investigating the Patterns and Dynamics of Urban Green Space in China’s 70 Major Cities Using Satellite Remote Sensing. *Remote Sensing*, 12, 1929, https://doi.org/10.3390/rs12121929.

Li, X., and Coauthors, 2020: Mapping global urban boundaries from the global artificial impervious area (GAIA) data. *Environ. Res. Lett.*, 15, 094044, https://doi.org/10.1088/1748-9326/ab9be3.

Liao, Y., Q. Zhou, and X. Jing, 2021: A comparison of global and regional open datasets for urban greenspace mapping. *Urban Forestry & Urban Greening*, 62, 127132, https://doi.org/10.1016/j.ufug.2021.127132.

Qiao, Z., L. Liu, Y. Qin, X. Xu, B. Wang, and Z. Liu, 2020: The Impact of Urban Renewal on Land Surface Temperature Changes: A Case Study in the Main City of Guangzhou, China. *Remote Sensing*, 12, 794, https://doi.org/10.3390/rs12050794.

Richards, D. R., and R. N. Belcher, 2019: Global Changes in Urban Vegetation Cover. *Remote Sensing*, 12, 23, https://doi.org/10.3390/rs12010023.

Yin, J., P. Fu, A. Cheshmehzangi, Z. Li, and J. Dong, 2022: Investigating the Changes in Urban Green-Space Patterns with Urban Land-Use Changes: A Case Study in Hangzhou, China. *Remote Sensing*, 14, 5410, https://doi.org/10.3390/rs14215410.

Zhang, P., C. Lin, S. Guo, W. Zhang, H. Fang, and P. Du, 2023: A labor-free index-guided semantic segmentation approach for urban vegetation mapping from high-resolution true color imagery. *International Journal of Digital Earth*, 16, 1640–1660, https://doi.org/10.1080/17538947.2023.2207839.